



**Superconducting Gamma/Neutron Spectrometer  
Task 1 Completion Report  
Evaluation of Candidate Neutron-Sensitive Materials**

**Z. W. Bell  
V. E. Lamberti  
BWXT Y-12, L.L.C.**

**A. Burger  
Fisk University**

**Date of Issue: June 20, 2002**

**Y-12  
NATIONAL  
SECURITY  
COMPLEX**

**Prepared by the  
Y-12 National Security Complex  
P. O. Box 2009,  
Oak Ridge, Tennessee 37831-8169  
managed by  
BWXT Y-12 L.L.C.  
for the  
U.S. DEPARTMENT OF ENERGY  
under contract DE-AC05-00OR-22800**

**MANAGED BY  
BWXT Y-12, L.L.C.  
FOR THE UNITED STATES  
DEPARTMENT OF ENERGY**

#### DISCLAIMER

This report was prepared as an account of work sponsored by an agency of the United States Government. Neither the United States Government nor any agency thereof, nor any of their employees, makes any warranty, express or implied, or assumes any legal liability or responsibility for the accuracy, completeness, or usefulness of any information, apparatus, product, or process disclosed, or represents that its use would not infringe privately owned rights. Reference herein to any specific commercial product, process or service by trade name, trademark, manufacturer, or otherwise, does not necessarily constitute or imply its endorsement, recommendation, or favoring by the United States Government or any agency thereof. The views and opinions of authors expressed herein do not necessarily state or reflect those of the United States Government or any agency thereof.

#### COPYRIGHT NOTICE

The submitted manuscript has been authored by a subcontractor of the U.S. Government under contract DE-AC0500OR-22800. Accordingly, the U.S. Government retains a paid-up, nonexclusive, irrevocable, worldwide license to publish or reproduce the published form of this contribution, prepare derivative works, distribute copies to the public, and perform publicly and display publicly, or allow others to do so, for U.S. Government purposes.

**Superconducting Gamma/Neutron Spectrometer  
Task 1 Completion Report  
Evaluation of Candidate Neutron-Sensitive Materials**

**Z. W. Bell  
V. E. Lamberti  
BWXT Y-12, L.L.C.**

**A. Burger  
Fisk University**

**Date of Issue: June 20, 2002**

**Prepared by the  
Y-12 National Security Complex  
P. O. Box 2009,  
Oak Ridge, Tennessee 37831-8169  
managed by  
BWXT Y-12 L.L.C.  
for the  
U.S. DEPARTMENT OF ENERGY  
under contract DE-AC05-00OR-22800**

Superconducting Gamma/Neutron Spectrometer  
Task 1 Completion Report  
Evaluation of Candidate Neutron-Sensitive Materials  
Z. W. Bell, V. E. Lamberti  
BWXT Y-12, LLC  
A. Burger  
Fisk University

## Executive Summary

A review of the scientific literature regarding boron- and lithium-containing compounds was completed. Information such as Debye temperature, heat capacity, superconductivity properties, physical and chemical characteristics, commercial availability, and recipes for synthesis was accumulated and evaluated to develop a list of neutron-sensitive materials likely to perform properly in the spectrometer. The best candidate borides appear to be  $\text{MgB}_2$  (a superconductor with  $T_c = 39$  K),  $\text{B}_6\text{Si}$ ,  $\text{B}_4\text{C}$ , and elemental boron; all are commercially available. Among the lithium compounds are  $\text{LiH}$ ,  $\text{LiAl}$ ,  $\text{Li}_{12}\text{Si}_7$ , and  $\text{Li}_7\text{Sn}_2$ . These materials have or are expected to have high Debye temperatures and sufficiently low heat capacities at 100 mK to produce a useful signal. The responses of  $^{10}\text{B}$  and  $^6\text{Li}$  to a fission neutron spectrum were also estimated. These demonstrated that the contribution of scattering events is no more than 3% in a boron-based system and 1.5% in a lithium-based system.

## Introduction

This project is concerned with the development of materials for use in a cryogenic neutron spectrometer and is complementary to work in progress by Labov<sup>1</sup> at LLNL to develop a cryogenic gamma ray spectrometer. Refrigeration to 100 mK lowers the heat capacity of these materials to the point that the energy of absorbed gamma and x rays, nuclei scattered by fast neutrons, and ions from  $(n, \alpha)$  reactions produce a measurable heat pulse, from which the energy of the incident radiation may be deduced. The objective of this project is the discovery, fabrication, and testing of candidate materials with which a cryogenic neutron spectrometer may be realized.

Neutron spectroscopy with a cryogenic detector will, of necessity, rely on reactions in which the incident neutron is absorbed, no or only a few gammas are emitted, and whose reaction products have short range. The first and third conditions guarantee that the heat pulse will be proportional to the sum of the kinetic energy and the  $Q$  value of the reaction. The second condition implies that the response function will not be very complicated. Taken together, these prevent determination of incident neutron energy with  $(n, \gamma)$  and scattering reactions. The former are disqualified because the necessarily small detector volume cannot capture the energy lost to gamma rays, while the latter are disqualified because scattering produces recoil ions with energies that depend on both the incident neutron's energy and the angle through which it is scattered. Since the scattered neutron is not captured or sensed, its information is lost, preventing recovery of the incident energy.

The ideal reactions for neutron spectroscopy are therefore seen to be those resulting in charged particles. In addition, the reaction products should have sufficiently simple structures that their production in excited states is either forbidden by conservation of energy or only occurs with a few different  $Q$  values. Fission in actinides, while seemingly excellent candidate reactions because of the tremendous energy and short range of the fragments, must be rejected because in addition to the fragments a significant amount of energy is radiated away as prompt neutrons and gammas. In addition, the fragments are typically nuclei with complex structures, leading to an abundance of possible  $Q$  values. Instead, the simple reactions in  $^3\text{He}$ ,  $^{10}\text{B}$ , and  $^6\text{Li}$  are the most promising.

Of these three candidate nuclei, helium must be discarded because it does not form compounds and the  $Q$  value for the  $(n,\alpha)$  reaction is 764 keV. With this low  $Q$  value, and only mass 3, pulses caused by the elastic scattering of MeV neutrons would be indistinguishable from those caused by thermal captures. Furthermore, containment of a useful quantity of  $^3\text{He}$  would be difficult. On the other hand, the masses of boron and lithium, the  $Q$ s of the capture reactions, and the energies of the first few excited states allow the separation of capture events from scattering events based on pulse height. Therefore, the initial search for candidate materials has concentrated here.

The chemistry of boron is well known. It forms a number of borides with the mass fraction of boron in excess of 20%, many of which are commercially available. In addition, elemental boron is stable, non-reactive, and commercially available. Although some of the borides might pose health hazards, all are solids and easily contained.

Lithium metal is somewhat more reactive than boron and it, too, forms many alloys and compounds. Most of these are reactive in the presence of water or water vapor, and will therefore need to be contained. Unfortunately, because lithium is so light, its mass fraction in most materials is insufficiently high for this application.

The remainder of this report gives the details of the investigation of the physical and chemical properties of boron and lithium compounds. In addition, the expected response of both boron and lithium neutron detectors to an incident fission neutron spectrum was estimated in order to determine the relative contributions of capture and scattering.

### **Estimate of Responses**

For simplicity, the fission neutron spectrum was modeled with a Maxwellian distribution as

$$p(E)dE = \frac{2}{1.36^{3/2}\pi^{1/2}} E^{1/2} e^{-E/1.36} dE$$

with  $E$  in MeV. The temperature 1.36 MeV was selected as representative of the neutron-induced fission process, and the differences in temperature among various isotopes do not affect the results significantly.

$^{10}\text{B}$  and  $^6\text{Li}$  neutron cross sections were obtained from the ENDF/B-VI<sup>2</sup> and BROND-2<sup>3</sup> compilations available from the National Nuclear Data Center<sup>4</sup> (NNDC) at Brookhaven National Laboratory. NNDC also tabulates nuclear structure data in the ENSDF files, which were used to obtain the energies of the first two excited states of each isotope.

Both boron and lithium have reactions in which energetic ions are produced. In the case of lithium, the  $^6\text{Li}(n, \alpha)t$  reaction produces an alpha particle and triton that share 4.78 MeV (the  $Q$  value of the reaction) in addition to the incident neutron's energy. The  $^{10}\text{B}(n, \alpha)^7\text{Li}$  reaction has two branches, with 94% of the reactions (at least at thermal energies) leaving  $^7\text{Li}$  in its first excited state (0.478 MeV) and 6% leaving  $^7\text{Li}$  in its ground state. The  $Q$  values for these reactions are 2.31 and 2.792 MeV, respectively. Since the reaction products have very short range and their entire kinetic energy will be captured in the detector material, the energy of the incident neutron can be recovered.

Since scattering of high-energy neutrons can also produce recoiling ions with energies comparable to those of absorption reaction products, the heat-pulse spectrum may or may not (depending on the mass of the target, energy of incident neutron, and energies of excited states of the target) be seriously contaminated with non-absorption events. It is, therefore, necessary to understand the distribution of recoil ions from an analysis of the kinematics of a non-relativistic neutron scattering from a target nucleus of mass number  $A$  at rest. The analysis requires no more than conservation of momentum and energy. In the laboratory frame

$$\begin{aligned} \text{Energy: } E_n &= E'_n + E_R - Q \\ \text{Longitudinal momentum: } p_n &= p'_n \cos(\mathbf{q}) + p_R \cos(\mathbf{j}) \\ \text{Transverse momentum: } 0 &= p'_n \sin(\mathbf{q}) - p_R \sin(\mathbf{j}) \\ E_n &= \frac{p_n^2}{2m}, \quad E'_n = \frac{p_n'^2}{2m}, \quad E_R = \frac{p_R^2}{2Am} \end{aligned}$$

where  $m$  is mass of a neutron,  $Am$  is taken to be the mass of the target,  $Q$  is positive for exothermic reactions (e.g., for the  $^6\text{Li}(n, \alpha)$  reaction,  $Q = 4.78$  MeV) and negative for scattering from excited states of the target nucleus,  $\theta$  is the scattering angle of the neutron, and  $\phi$  is the angle of recoil of the target. The incident neutron has energy  $E_n$  and momentum  $p_n$ , the outgoing neutron has energy  $E'_n$  and momentum  $p'_n$ , and the recoiling target has energy  $E_R$  and momentum  $p_R$ . Elimination of  $\phi$ ,  $p_R$ ,  $p_n$ ,  $E'_n$ , and  $p'_n$  yields a quadratic equation for  $E_R$  in terms of  $\theta$ ,  $E_n$ , and  $Q$ :

$$\left( (A+1)E_R - Q - 2E_n \right)^2 + 4E_n(E_R - Q - E_n) \cos^2(\theta) = 0 \quad (1)$$

Since  $E_R$  is maximized at  $\theta = \pi$ , at that angle equation 1 becomes

$$\left( (A+1)E_R - Q - 2E_n \right)^2 + 4E_n(E_R - Q - E_n) = 0 \quad (2)$$

For elastic scattering,  $Q = 0$  and the left hand side simplifies to

$$((A+1)^2 E_R - 4AE_n)E_R = 0$$

from which the solutions  $E_R = 0$  and

$$E_R = \frac{4A}{(A+1)^2} E_n \quad (3)$$

are found.  $E_R = 0$  corresponds to  $\theta = 0$ , for which  $\cos^2$  is also unity. For  $Q > 0$ , the maximum recoil energy is found from equation (2):

$$E_R = \frac{2A}{(A+1)^2} E_n \left[ 1 + \frac{(A+1)Q}{2A E_n} + \sqrt{1 + \frac{A+1}{A} \frac{Q}{E_n}} \right] \quad (4)$$

Values of  $Q < 0$  apply to scattering that leaves the target nucleus in an excited state with energy  $Q$ . The value of the discriminant leads to three possible scenarios in this case. If  $E_n < -\frac{A+1}{A}Q$ , then there is insufficient energy to leave the target nucleus in a state with excitation energy  $Q$ , and only elastic scattering and scattering from lower lying states are permitted. At

$E_n = -\frac{A+1}{A}Q$ , the scattered neutron and excited recoiling nucleus are at rest in the center of

momentum frame and the ion has energy  $E_R = \frac{A}{(A+1)^2} E_n$  in the laboratory. For  $E_n > -\frac{A+1}{A}Q$ ,

scattering events are energetically allowed that leave the recoiling nucleus in an excited state with energy  $Q$ .

Calculations were performed using the above analysis to estimate the deposition of energy in both  $^{10}\text{B}$  and  $^6\text{Li}$ . Absorption and scattering cross sections were multiplied by the Maxwellian distribution to obtain a quantity,  $s(E_n)p(E_n)$ , proportional to the probability of each kind of interaction, and the maximum deposited energy for each reaction was computed as a function of  $E_n$ .  $s(E_n)p(E_n)$  was then plotted as a function of maximum deposited energy. For each isotope, scattering from the first two excited states and the  $(n, \alpha)$  reaction were considered.

Of interest also is the minimum neutron energy required to produce an excited recoiling target nucleus with kinetic energy equal to the  $Q$  value,  $Q_{\text{abs}}$ , of the absorption reaction. Substituting  $E_R = Q_{\text{abs}}$  in equation (2) leads to

$$E_n = \frac{((A+1)Q_{\text{abs}} - Q)^2}{4AQ_{\text{abs}}} \quad (5)$$

For  $Q = 0$ , equation (5) reduces to equation (3).

Clearly, the minimum neutron energy required to generate a recoil with energy  $Q_{\text{abs}}$  occurs when  $Q = 0$ . For  $A$  large compared to unity, Equation (5) predicts  $E_n \sim 0.25(A+1)Q_{\text{abs}}$ . Consequently, even for relatively light materials such as oxygen, aluminum, and magnesium, neutrons in excess

of 8 MeV are required. Since neutrons in excess of this energy have a probability of production below 1%, scattering from materials other than boron and lithium have been ignored.

### Boron

Figure 1 shows the maximum recoil energy as a function of incident neutron energy for scattering from the ground and first two excited states of  $^{10}\text{B}$ . Note the suppressed zero on the x-axis.

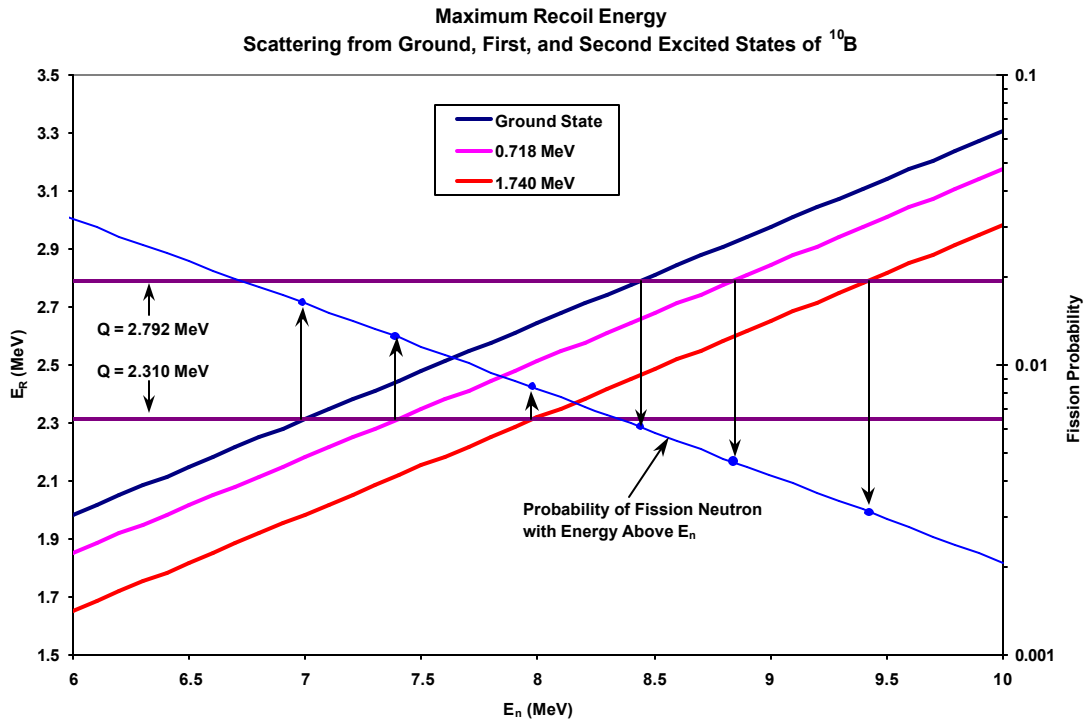


Figure 1. Maximum energy of recoiling boron ion.

The two horizontal lines represent the two values of  $Q_{\text{abs}}$  corresponding to leaving  $^7\text{Li}$  in its ground and first excited state (478 keV). The blue line is the probability of the occurrence of neutrons with energy greater than  $E_n$  under the assumption of a Maxwellian distribution with temperature 1.36 MeV. The probability scale is logarithmic and at the right of the figure. The arrows identify  $E_n$  at which the recoil energy equals  $Q_{\text{abs}}$  and the probability of the presence of a fission neutron at least as energetic as required.

It is seen that approximately 7 MeV is required to produce a recoiling  $^{10}\text{B}$  with 2.31 MeV. This means that a 7 MeV neutron undergoing a head-on collision with a boron nucleus will produce a recoil that will deposit the same energy as would occur if a thermal neutron were captured by boron. Absorption and scattering would be indistinguishable in this case and confuse the analysis of a pulse height spectrum. However, it is also seen that neutrons with at least this energy are expected to occur with a probability of only 1.6%. Consequently, scattering is expected to be a negligible effect.

Figure 2 shows the relative contributions of capture and scattering in  $^{10}\text{B}$ . The figure plots the product of the cross section and the fission neutron energy distribution as a function of the energy of the reaction products. For the capture reaction, the energy of the reaction products is simply  $Q_{\text{abs}} + E_n$ ; for the scattering reactions, it is the energy of the recoiling boron nucleus. For the purposes of developing an upper bound, the worst case of maximum recoil energy was assumed.

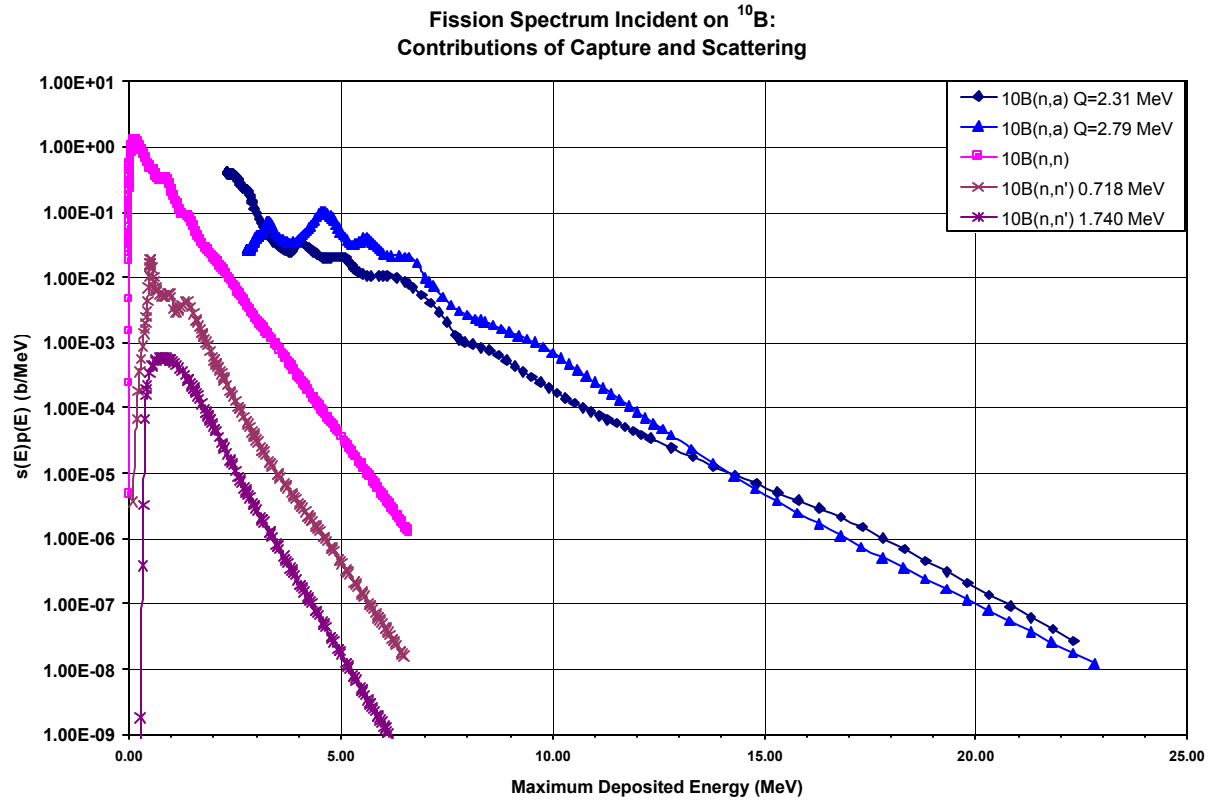


Figure 2. Relative contribution of scattering and capture events in boron

Each curve was calculated for incident neutrons from 0 to 20 MeV; the scattering curves end between 6 and 7 MeV because that is the maximum recoil energy that can be imparted to a  $^{10}\text{B}$  nucleus. Note the logarithmic ordinate and linear abscissa.

It is seen that elastic scattering is the dominant interference in the expected response. However, the number of available neutrons above 7 MeV is sufficiently small that it represents at most only about a 3% effect. In other words, by placing a threshold at 2.31 MeV and assuming that all events producing pulses with heights above that threshold are caused by absorption, no more than 3% of those events will be caused by misclassified scatterings.

The presence of the two capture reactions is easily handled by referring to the kinematics of the capture reactions. For each pulse height (*i.e.* deposited energy),  $E$ , the response contains either only a contribution from reaction leaving  $^7\text{Li}$  in its first excited state, or contributions from both reactions, with neutrons differing in energy by 480 keV. That is,

$$2.31 \leq E \leq 2.79 \text{ MeV} : S(E) \propto \Phi(E - 2.31) s_1(E - 2.31)$$

$$2.79 \text{ MeV} \leq E : S(E) \propto \Phi(E - 2.31) s_1(E - 2.31) + \Phi(E - 2.79) s_0(E - 2.79)$$

It is seen that the ground state contribution is generated by neutrons with energies 480 keV **below** those generating the first excited state contribution. Thus, a spectrum stripping analysis procedure suggests itself: The neutron spectrum up to 480 keV is determined entirely by the deposited energy spectrum between 2.31 and 2.79 MeV. The measured data at 2.79 MeV is generated by 480 keV neutrons leaving  ${}^7\text{Li}$  in the first excited state, and by thermal neutrons leaving  ${}^7\text{Li}$  in its ground state. Since the thermal flux will have been determined from the data at 2.31 MeV, the ground state contribution can be calculated and subtracted from the measured spectrum, yielding the flux at 480 keV. Similarly, the flux of 500 keV neutrons is calculated by subtracting the ground state contribution caused by the already determined flux at 20 keV from the measured data at 2.81 MeV. This procedure is iterated through the entire measured spectrum. The usual pitfalls associated with spectrum stripping do not apply to this procedure since in contrast to conventional pulse height data, stripping here proceeds from a region of high counts to a region of low counts. Therefore, the situation of small differences between large numbers is not expected to occur and the resulting uncertainties should be well behaved.

### Lithium

The situation in lithium is less complicated because of the single value of  $Q_{\text{abs}}$ . Figure 3 shows maximum recoil energy for scattering from the ground and first two excited states of  ${}^6\text{Li}$ . Note the suppressed zero on the x-axis.

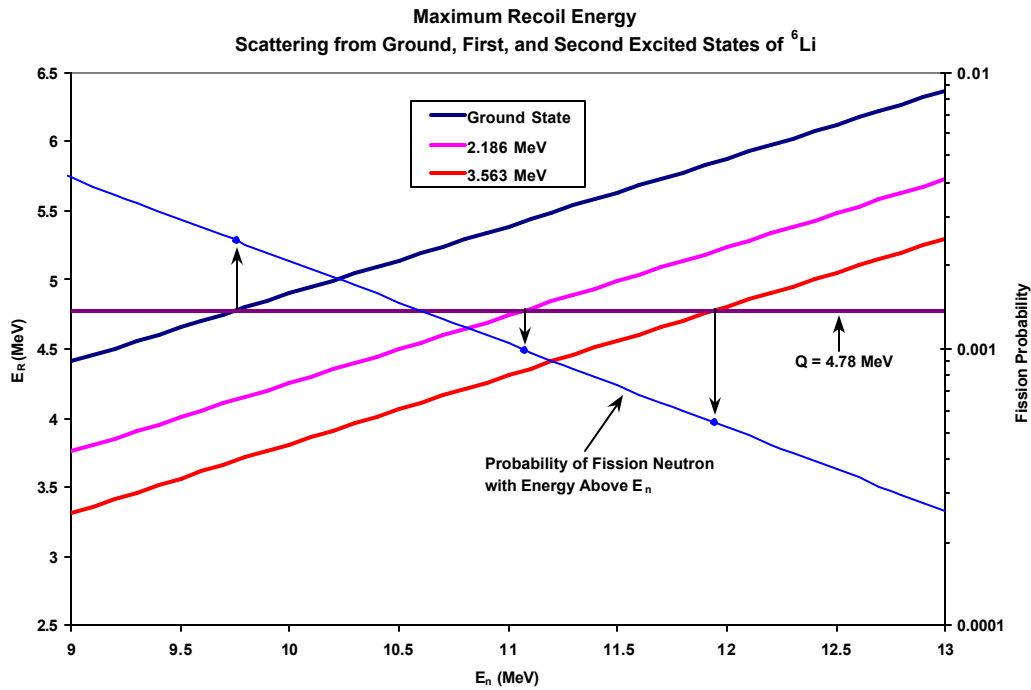


Figure 3. Maximum recoil energy from scattering from lithium.

It is immediately apparent that because of the higher  $Q$  value of the  $(n,\alpha)$  reaction and the lower weight of  ${}^6\text{Li}$ , neutrons with energy in excess of 9.5 MeV are need to produce scattered ions with energy equal to the  $Q$  value. The probability of the occurrence of these neutrons (assuming a Maxwellian distribution) is an order of magnitude lower than that for corresponding neutrons in the case of boron. This fact and the higher  $Q$  value are reflected in the improved capture-to-scattering fraction seen in Figure 4.

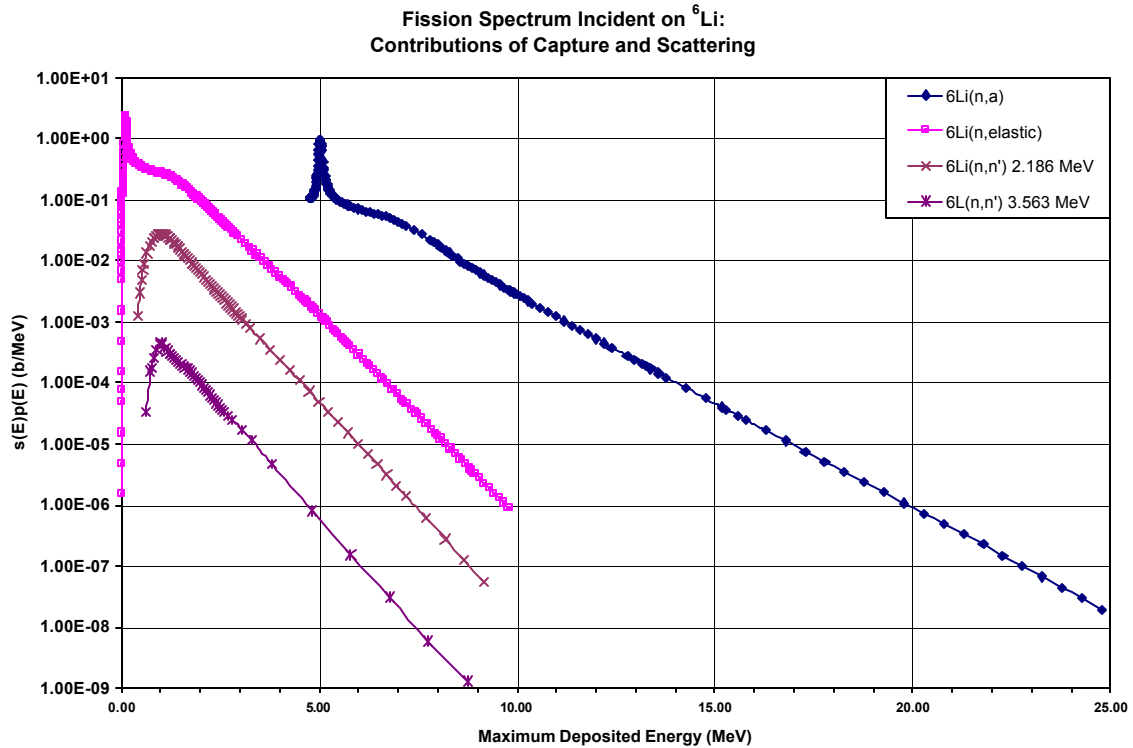


Figure 4. Response of lithium system to fission neutrons

As in the case of boron, each curve was calculated for neutrons up to 20 MeV. Note the logarithmic scale. The data for the contribution from scattering processes ends near 10 MeV deposited energy because of the kinematics of the lighter  ${}^6\text{Li}$ -n system. The spike near 120 keV in the elastic scattering data and near 5 MeV in the capture data arises from the resonance in the  ${}^6\text{Li}$  cross section near 240 keV.

The lithium data indicate that placing a threshold at 4.78 MeV will cause only about 1% of the spectrum to contain misclassified scattering events. Scattering from the excited states of lithium is over an order of magnitude smaller than elastic scattering.

## Criteria for Detector Materials

Labov's<sup>1</sup> detector is a microcalorimeter constructed from a millimeter-scale absorber and a transition-edge-sensor\* (TES) thermometer. The energy resolution of a device of this type is determined by thermal fluctuations and Johnson noise, and is given by

$$\Delta E = 2.35 \mathbf{x} \sqrt{k_B T_{op}^2 C},$$

where  $k_B$  is Boltzmann's constant,  $T_{op}$  is the operating temperature in degrees Kelvin,  $C$  is the total heat capacity, and  $\mathbf{x}$  is a parameter dependent upon the sensitivity of the thermometer and the operating conditions.<sup>1,5</sup> Small values of  $\Delta E$ , or high qualities of energy discrimination, thus correspond to small values of  $T_{op}$  and  $C$ . Labov *et al.*<sup>1</sup> typically work near 60 mK with a detector exhibiting a total heat capacity *ca.* 80 keV/mK ( $12.8 \times 10^{-12} \text{ J K}^{-1}$ ); using a superconducting Sn absorber, the LLNL group has detected pulses resulting from absorption of 60 keV gamma rays with a resolution of 70 eV.

At low temperatures, the total heat capacity of a non-magnetic, non-superconducting material can usually be approximated as

$$C = \mathbf{g}T + \mathbf{b}T^3,$$

in which the first and second terms represent the electronic and lattice heat capacities, respectively,  $T$  is the absolute temperature, and  $\mathbf{g}$  and  $\mathbf{b}$  are material-dependent constants.<sup>6</sup> In the free-electron approximation,

$$\mathbf{g} = \frac{\mathbf{p}}{2T_F} n k_B,$$

where  $T_F$  is the Fermi temperature (typically  $10^5$  K) and  $n$  is the concentration of "free" charge carriers; in the low-temperature limit of the Debye model of the lattice heat capacity,

$$\mathbf{b} = \frac{12\mathbf{p}^4}{5} R \left( \frac{1}{\mathbf{q}_D} \right)^3,$$

where  $\mathbf{q}_D$  is the Debye temperature and  $R$  is the universal gas constant. The quantities  $n$  (or  $\mathbf{g}$ ) and  $\mathbf{q}_D$  are tabulated for most elements and many compounds, and can be estimated by a variety of means. Thus, the search for neutron detector materials with sufficiently small heat capacities can be restated in terms of sufficiently small values of  $\mathbf{g}$  and  $\mathbf{b}$ .

---

\* The TES is a bi- or multi-layer structure composed of alternating superconducting and non-superconducting films; due to the well-known superconductor proximity effect, the entire device enters the superconducting state at a transition temperature determined by the compositions and widths of the layers. In practice, the TES is held near the narrow temperature transition between the superconducting and normal states, so that the small increase in temperature resulting from absorption of a photon causes a large change in resistance.

The Debye temperatures of most solids are greater than 100 K and can, although rarely do, exceed 2000 K; in general, larger values of  $q_D$  are associated with stiffer materials. Because of the inverse cubic dependence of  $\mathbf{b}$  upon  $q_D$ , and the small dimensions of the absorber ( $1 \times 1 \times 0.25 \text{ mm}^3$  in the current configuration), even a material with a relatively small Debye temperature may provide an acceptably low lattice heat capacity at operating temperatures less than 1 K. Our candidate neutron detector materials typically have Debye temperatures several times greater than the value for the current choice of elemental tin (260 K<sup>7</sup>).

The magnitude of  $n$  is somewhat more critical since both  $\gamma$  and the electron heat capacity scales linearly with this variable. For materials with essentially no free charge carriers at sub-Kelvin temperatures, like insulators and intrinsic and lightly-doped semiconductors,  $\mathbf{g}$ , and with it the electronic contribution to the heat capacity, are negligible at typical values of  $T_{op}$ . For metals and heavily-doped semiconductors, on the other hand,  $\mathbf{g}$  can be of the order of  $1 \text{ mJ mol}^{-1} \text{ K}^{-2}$  (and even much greater for the so-called “heavy-fermion” materials). The measured value of  $\mathbf{g}$  for lithium metal,<sup>8</sup> for instance, is  $1.63 \text{ mJ mol}^{-1} \text{ K}^{-2}$ . ( $\mathbf{b} = 0.031 \text{ mJ mol}^{-1} \text{ K}^{-4}$  for Li with  $q_D = 400 \text{ K}$ .<sup>7</sup>) At first glance, therefore, we might conclude that we must discard conductors as a whole because their electronic heat capacities are intolerably large. However, for a *superconductor* well below its critical temperature ( $T_c$ ), the linear electronic contribution to the heat capacity is replaced by a term that vanishes exponentially with decreasing temperature. The BCS theory provides the estimate

$$C_{es} \approx 9.17 \mathbf{g} T_c \exp\left(-\frac{1.5 T_c}{T}\right)$$

for  $T \rightarrow 0$ , which predicts values far below those of a normal metal at low temperatures.<sup>9</sup> Thus, we also consider conductors if they display a superconducting transition temperature suitably above  $T_{op}$ . The low-temperature allotrope of elemental tin — “grey” tin, stable at temperatures less than  $13.2^\circ\text{C}$  — is a narrow-gap semiconductor ( $E_g = 0.082 \text{ eV}$  at  $0 \text{ K}$ <sup>10</sup>) that displays Type I superconductivity with  $T_c = 3.7 \text{ K}$ .<sup>11</sup>

In addition, we placed a number of other chemical, engineering, and safety constraints on potential detector materials:

- Weight percentage of  $^6\text{Li}$  or  $^{10}\text{B}$  exceeding 20%;
- Density exceeding  $2 \text{ g cm}^{-3}$ ;
- Stability in air at room temperature;
- Robustness toward thermal cycling to sub-Kelvin temperatures;
- Commercial availability for trial experiments; and
- No toxic, radiological, or explosive hazards.

We expect that the desired robustness toward deep thermal cycling will be most easily achieved through utilization of single crystals. As we move beyond the concept-proving experiments, the restriction on commercial availability will certainly be relaxed for an exceptionally promising candidate; indeed, we briefly describe such a material below.

## Candidate ${}^6\text{Li}$ - or ${}^{10}\text{B}$ -loaded Detector Materials

All other considerations being equal, we would prefer a detector based on  ${}^6\text{Li}$  since the  $Q$ -value of this isotope is somewhat more favorable than that of  ${}^{10}\text{B}$ .<sup>12</sup> Unfortunately, with the exception of lithium fluoride ( $q_D = 730 \text{ K}^{13}$ ), which has already been used in bolometers for neutron detection<sup>14</sup> and in experiments designed to detect dark matter,<sup>15</sup> we have found it very difficult to identify candidates that satisfy even most of our material specifications. Lithium metal, for example, has a quite acceptable Debye temperature of 400 K,<sup>7</sup> but is toxic and so reactive toward atmospheric water that it would require encapsulation; in addition, it is a good conductor, but does not exhibit superconductivity to temperatures as low as 5 mK.<sup>16</sup> Therefore, we do not propose any Li-bearing compounds for the first round of experiments. We have, however, identified three promising alloy systems for a second round of screening experiments — aluminum-lithium, lithium-silicon, and lithium-tin — each of which exhibits a eutectic on the midpoint (Al-Li) or lithium-heavy side of the join. Aluminum and tin are known superconductors and it is possible that their alloys with lithium will exhibit superconductivity as well at the eutectic compositions. Among lithium-containing insulators, LiH may hold promise. It has both a high Debye temperature (815 or 920 K<sup>17</sup>) and a high concentration of lithium; however, it is reported to be corrosive, reactive, and flammable,<sup>18</sup> and thus would require encapsulation.

On the other hand, we have been able to find quite a few  ${}^{10}\text{B}$ -loaded materials that satisfy most if not all of our requirements; these are summarized in table below. All are available from commercial vendors in a variety of forms. The first choice is clearly  $\text{MgB}_2$ , since this material is characterized by excellent values of boron content (45.5%) and Debye temperature ( $750 \pm 30 \text{ K}^{19}$ ), poses no hazards for users, and is stable in the presence of atmospheric water, oxygen, and carbon dioxide at room temperature. In addition, it exhibits superconductivity below 39 K and a number of recipes have been published for synthesis of single crystals.<sup>20</sup> Moreover, we expect that the knowledge base for  $\text{MgB}_2$  will increase rapidly in the immediate future because it is currently under intense scrutiny as the holder of the highest  $T_c$  reported to date for a non-oxide or non- $\text{C}_{60}$ -based superconductor.<sup>21</sup>

We also intend to test, in rough order of preference, elemental boron,  $\text{B}_4\text{C}$ , and  $\text{B}_6\text{Si}$  in our first round of experiments. All of these materials have measured or estimated Debye temperatures greater than 1000 K and all are semiconductors. They are not known superconductors, but the possibility exists that one or more of these phases might be superconducting at the operating temperature of the Labov instrument; our first series of screening heat capacity measurements, extending to *ca.* 0.5 K, will provide a first answer to this question.

Moving beyond the restrictions described above, and beyond the first round of experiments, we find the so-called *higher borides* of several elements to be possibilities for detector materials. One particularly intriguing example is  $\text{B}_{12}\text{S}$ , a boron-carbide-like material that exhibits high chemical and thermal stability and becomes superconducting below 0.39 K.<sup>22</sup>  $\text{B}_{12}\text{S}$  does not appear to be commercially available, but may be prepared through a procedure described by Matkovich.<sup>23</sup> The hexaborides of Y and several of the lanthanides have superconducting transition temperatures and boron contents well within our limits, and some are commercially

available; the  $T_c$  of  $YB_6$  is 7.1 K and, for example, the  $T_c$  of  $LaB_6$  is 5.7 K.<sup>24</sup> Other higher borides of interest include  $AlB_{12}$ ,  $ScB_{12}$ ,  $Sc_{11}B_{305}$ ,  $MgB_4$ ,  $MgB_7$ , and  $TiB_{12}$ .

**Table 1. Promising  $^{10}B$ -loaded Neutron Detector Materials**

| Phase   | Wt.% $^{10}B$ | $r^a$<br>$g\ cm^{-3}$ | $q_D$<br>K        | SC $T_c$<br>K        | Hazards  | Reactivity at RT                     |
|---------|---------------|-----------------------|-------------------|----------------------|--|--------------------------------------|
| $AlB_2$ | 42.6          | 3.19                  | Unknown           | Note <sup>b</sup>    | Irritant   | Stable; avoid acids                  |
| B       | 100           | 2.34                  | 1250 <sup>c</sup> | (1.3 <sup>d</sup> )  | Irritant<br>Powder flammable<br>Harmful if inhaled/swallowed | Stable                               |
| BN      | 41.7          | 2.18                  | 1900 <sup>a</sup> | (1.28 <sup>e</sup> ) | Irritant<br>Harmful if inhaled                               | Stable; avoid strong acids/oxidizers |
| $B_4C$  | 76.9          | 2.50                  | 1850 <sup>f</sup> | (1.28 <sup>e</sup> ) | Harmful if inhaled   | Stable                               |
| $B_6Si$ | 68.1          | 2.47                  | 1650 <sup>f</sup> | Unknown              | N/A  | Stable                               |
| $MgB_2$ | 45.5          | 2.57                  | $750 \pm 30^g$    | 39 <sup>h</sup>      | N/A  | Stable; avoid acids                  |
| $ScB_2$ | 30.8          | 3.17                  | 550 <sup>i</sup>  | Unknown              | Unknown  | Unknown                              |
| $TiB_2$ | 29.5          | 4.38                  | 820 <sup>i</sup>  | (0.3 <sup>j</sup> )  | N/A  | Stable; avoid oxidizers              |

Notation:  $r$ , density;  $q_D$ , Debye temperature; SC  $T_c$ , superconducting critical temperature. Critical temperatures given in parentheses indicate the lowest temperature at which superconductivity has not been observed.

<sup>a</sup>*Handbook of Chemistry and Physics*, 78<sup>th</sup> edition; Lide, D. R., Ed.; CRC Press: New York, 1997.

<sup>b</sup>Bulk superconducting transition disappears for  $x \geq 0.3$  in  $Mg_{1-x}Al_xB_2$  ( $0 \leq x \leq 0.4$ ): Slusky, J. S.; Rogado, N.; Regan, K. A.; Hayward, M. A.; Khalifah, P.; He, T.; Inumaru, K.; Loureiro, S. M.; Haas, M. K.; Zandbergen, H. W.; Cava, R. J. *Nature* **2001**, *410*, 343.

<sup>c</sup>de Launay, J. In *Solid State Physics*; vol. 2; Seitz, F., Turnbull, D., Eds.; Academic Press: New York, 1956.

<sup>d</sup>Matthias, B. T. In *Progress in Low Temperature Physics*; vol. 2; Gorter, C. J., Ed.; North Holland: Amsterdam, 1957.

<sup>e</sup>Matthias, B. T.; Hulm, J. K. *Phys. Rev.* **1952**, *87*, 799.

<sup>f</sup>Estimated according to Siethoff, H. *Intermetallics* **1997**, *5*, 625.

<sup>g</sup>Bud'ko, S. L.; Lapertot, G.; Petrovic, C.; Cunningham, C. E.; Anderson, N.; Canfield, P. C. *Phys. Rev. Lett.* **2001**, *86*, 1877.

<sup>h</sup>Nagamatsu, J.; Nakagawa, N.; Muranaka, T.; Zenitani, Y.; Akimitsu, J. *Nature* **2001**, *410*, 63.

<sup>i</sup>Castaing, J.; Caudron, R.; Toupance, G.; Costa, P. *Solid State Comm.* **1969**, *7*, 1453.

<sup>j</sup>Agrestini, S.; Di Castro, D.; Sansone, M.; Saini, N. L.; Saccone, A.; De Negri, S.; Giovannini, M.; Colapietro, M.; Bianconi, A. *J. Phys.: Condens. Matter* **2001**, *13*, 11689.

## References

- <sup>1</sup> Chow, D. T.; Lindeman, M. A.; Cunningham, M. F.; Frank, M.; Barbee Jr., T. W.; Labov, S. E. *Nucl. Instr. And Meth. A* **2000**, *444*, 196.
- <sup>2</sup> *Data Formats and Procedures Manual for Evaluated Nuclear Data File, ENDF-6, ENDF-102* (BNL-NCS-44945).
- <sup>3</sup> BROND-2.1, Russian Evaluated Nuclear Data Library, IAEA-NDS-90, Rev. 7 (1993).
- <sup>4</sup> <http://www.nndc.bnl.gov>.
- <sup>5</sup> Moseley, S. H.; Mather, J. C.; McCammon, D. *J. Appl. Phys.* **1984**, *56*, 1257.
- <sup>6</sup> Ashcroft, N. W.; Mermin, N. D. *Solid State Physics*; International Thompson Publishing: Belmont, CA, 1976, chaps. 2, 23.
- <sup>7</sup> *Ibid.*, p. 461.
- <sup>8</sup> Kittel, C. *Introduction to Solid State Physics*, 6<sup>th</sup> edition; Wiley: New York, 1986, p. 141.
- <sup>9</sup> Buchel, W. *Superconductivity: Fundamentals and Applications*; VCH: New York, 1991, p.101.
- <sup>10</sup> Sze, S. *Physics of Semiconductor Devices*, 2<sup>nd</sup> edition; Wiley: New York, 1981, p.849.
- <sup>11</sup> Ashcroft, N. W.; Mermin, N. D., *op. cit.*, p. 729.
- <sup>12</sup> Knoll, G. F. *Radiation Detection and Measurement*, 3<sup>rd</sup> edition; Wiley: New York, 1999, p. 507.
- <sup>13</sup> Ref 6, p. 459.
- <sup>14</sup> Silver, C. S; Beeman, J.; Timbie, P. T.; Zhou, J. W. *Nucl. Instr. and Meth. A*, to be published. A preprint can be found at <http://cmb.physics.wisc.edu/Neutron/revision.pdf>
- <sup>15</sup> Ootani, W.; Minowa, M.; Miuchi, K.; Watanabe, T.; Ito, Y.; Takeda, A.; Inoue, Y.; Ootuka, Y., *Nucl. Instr. and Meth. A* **1999**, *436*, 233.
- <sup>16</sup> <http://socrates.berkeley.edu/~davisgrp/lithium/paper/JLTP0998.pdf>.
- <sup>17</sup> <http://www.oxmat.co.uk/Crysddata/lih.htm>.
- <sup>18</sup> See, for example, the material safety data sheet published by Alfa Aesar at <http://www.alfa.com/>.
- <sup>19</sup> Bud'ko, S. L.; Lapertot, G.; Petrovic, C.; Cunningham, C. E.; Anderson, N.; Canfield, P. C. *Phys. Rev. Lett.* **2001**, *86*, 1877.
- <sup>20</sup> See, for example: Xu, M; Kitazawa, H.; Takano, Y.; Ye, J.; Nishida, K.; Abe, H.; Matsushita, A.; Tsujii, N.; Kido, G. *Appl. Phys. Lett.* **2001**, *79*, 2779.
- <sup>21</sup> <http://www.superconductors.org>
- <sup>22</sup> Leyarovska, L.; Leyarovski, E. *J Less Common Met.* **1979**, *67*, 249.
- <sup>23</sup> Matkovich, V. I. *J. Am. Chem. Soc.* **1961**, *83*, 1804.
- <sup>24</sup> Buzea, C.; Yamashita, T. *Supercond. Sci. Technol.* **2001**, *14*, R115.